

This item is the archived peer-reviewed author-version of:

Structured catalysts for methanol-to-olefins conversion : a review

Reference:

Lefevere Jasper, Mullens Steven, Meynen Vera, Van Noyen Jasper.- Structured catalysts for methanol-to-olefins conversion : a review

Chemical papers - ISSN 0366-6352 - Warsaw, De Gruyter Open Ltd, 68:9(2014), p. 1143-1153

Full text (Publishers DOI): <http://dx.doi.org/doi:10.2478/s11696-014-0568-0>

To cite this reference: <http://hdl.handle.net/10067/1176950151162165141>

Structured catalysts for methanol-to-olefins: a review

^{a,b} Jasper Lefevere, ^aSteven Mullens, ^bVera Meynen, ^aJasper Van Noyen

^a*Sustainable Materials Management, Flemish Institute for Technological Research - VITO,
Boeretang 200, B-2400 Mol, Belgium*

^b*Department of Chemistry, University of Antwerp, Universiteitsplein 1, B-2610 Antwerp,
Belgium*

Corresponding author: Dr. Ir., Jasper Van Noyen; jasper.vannoyen@vito.be; Boeretang 200,
B-2400 Mol, Belgium

Received [Dates will be filled in by the Editorial office]

The conversion of methanol to light olefins is a promising alternative for the conversion of new feedstocks such as gas, coal or biomass to ethylene and propylene, via methanol-to-olefins. During the last decade, structured catalysts have received increasing attention for this reaction. The effect of such structured catalysts on the stability and selectivity is discussed in this review. The reaction and coking mechanism show the importance of good mass transfer properties of the catalyst in the MTO reaction. Important aspects such as thickness of the coating, crystal size of the zeolite and architecture of the support on the mass transfer properties of the final catalyst are highlighted. An overview of the catalytic results of structured catalysts for the MTO reaction is presented.

Keywords: methanol-to-olefins, structured catalyst, zeolites, SAPO-34, ZSM-5

Introduction

For more than 50 years the thermal cracking of naphtha has been the major production process for ethylene and propylene. These two platform molecules are key intermediates in

34 the chemical industry. Using polymerization, oxidation, halogenation,... reactions they are the
35 building blocks of a whole range of products. The rise of shale gas technology in the US in
36 the past decades has led to the construction of ethane crackers as well as retrofitting of naphta
37 crackers, as ethane crackers are economically more favourable over naphta crackers. This
38 trend has resulted in an increasing shortage of propylene supply and an increasing attraction
39 for tuning the methanol-to-olefins (MTO) reaction towards higher propylene yield (Rahimi &
40 Karimzadeh, 2011; Yilmaz & Müller, 2009). The ever rising demand for light olefins,
41 specifically for propylene, combined with an increase in oil prices, are the main drivers for the
42 investigation for alternative methods for ethylene and propylene production. The conversion
43 of methanol to light olefins could offer an alternative process for light olefin production, due
44 to its higher selectivity towards propylene. Furthermore, the low CO₂ emissions increase the
45 appeal of the MTO technology (J. Q. Chen, Bozzano, Glover, Fuglerud, & Kvisle, 2005).
46 Methanol can be produced from alternative feedstocks with proven technologies such as
47 steam reforming of natural gas, gasification of coal or gasification of biomass (T Ren, Patel,
48 & Blok, 2008). The location of methanol production plays a crucial role in the economic
49 viability of the methanol to olefin technology. Most of the natural gas reserves are found in
50 remote locations and the transportation of this gas would not be economical. Converting this
51 stranded gas to higher value chemicals could be beneficial for the chemical industry (T Ren et
52 al., 2008; Tao Ren, Daniëls, Patel, & Blok, 2009). In addition, the MTO technology offers the
53 possibility for production of light olefins in regions with gas and coal reserves but without oil.
54 The Lurgi process for methanol-to-propylene (MTP) has been proven commercially viable in
55 China. Recently 3 plants using the Lurgi technology have started up for the production of
56 olefins from coal: Shenhua Ningxia Coal Industry Group (500 kton/year MTP, 2010);
57 Shenhua Group (Baotou) (600 kton/year MTO, 2010) and Datang International Power
58 Generation (460 kton/year MTP, 2011) (D. Chen, Moljord, & Holmen, 2012). Alternatively,
59 the UOP/Hydro MTO process developed by UOP and Norsk Hydro (now Ineos) has been
60 proven successful in the semi-commercial test-plant in Belgium in 2008 (TOTAL, 2008). The
61 test reactor uses an additional olefin cracking step for the production of propylene and
62 ethylene. After the MTO reaction all C₄+ products are lead to an additional cracking reactor.
63 By adjusting the operating conditions of this reactor the ethylene and propylene yield in this
64 process can be modified. Several plants combining the UOP/Hydro MTO process and the
65 Total Petrochemicals/UOP Olefin Cracking process for the production of light olefins from
66 methanol, synthesized from coal, are planned for four sites with an overall production
67 capacity of about 1.2 Mton/year (J. Q. Chen et al., 2005).

68 The conversion of methanol-to-olefins is catalyzed by zeolites, which are, to the best
69 of our knowledge, the only type of catalysts commercially used for MTO. The two most
70 commonly used zeolites in MTO processes are ZSM-5 (MFI-Type) and SAPO-34 (CHA-
71 Type). ZSM-5 is a medium sized pore aluminosilicate with 10-membered ring pores. In
72 general, it has a high selectivity towards propylene and butylene and a long catalyst life, but
73 with a lower yield of light olefins compared to SAPO-34. SAPO-34 is a
74 silicoaluminophosphate with small 8-membered ring pores. It has a high selectivity towards
75 ethylene but it suffers from fast deactivation due to coke formation (Chae, Song, Jeong, Kim,
76 & Jeong, 2010; J. Q. Chen et al., 2005; Li et al., 2011). The ZSM-5 zeolite is used in the
77 Lurgi process in a packed bed configuration, while the UOP/Hydro process uses SAPO-34 as
78 a catalyst in a fluidized bed configuration due to the fast deactivation. Operation in coupled
79 fluidized beds allows for continuous regeneration of the catalyst, analogous to an FCC
80 process. As several literature reviews deal with the general aspects of the different catalysts,
81 the operating conditions, the reaction mechanism and the deactivation of methanol to
82 hydrocarbons, they will not be discussed in great detail in this review and focus will be put on
83 the specific influence of using structured catalysts (D. Chen et al., 2012; Keil, 1999; McCann
84 et al., 2008; Olsbye et al., 2012; Sano, Kiyozumi, & Shin, 1992; Stöcker, 1999; Wender,
85 1996).

86 Structured catalytic reactors can offer great advantages over traditional packed
87 catalytic beds, as they combine a lower pressure drop with a high surface-to-volume ratio.
88 The catalyst is generally applied as a thin coated layer onto a support structure. This thin
89 coated layer in combination with the large pores of the structured packing reduces the
90 pressure drop over the reactor in comparison with a packed bed. The use of macroporous
91 structured catalysts can increase both the mass and heat transfer properties of a catalytic bed,
92 which is especially of interest in exothermic reactions such as MTO. Due to these important
93 benefits, the use of structured catalysts in the MTO reaction has received increasing attention
94 over the last years. This paper highlights some important properties of the reaction
95 mechanism and the selectivity of the reaction, as well as the progress made in recent years for
96 structured catalysts in MTO technology. The coating methods for depositing a thin zeolite
97 film on a structured support are summarized. The effect of mass transfer properties of
98 catalytic systems on the stability and selectivity of the reaction is highlighted. Both thickness
99 of the coating and the architecture of the support material influence the mass transfer
100 properties of the final catalyst. Their influence on the selectivity and stability are described in
101 detail, including the benefits and drawbacks of the use of a structured catalyst. Alternatively

102 to a coated catalyst, a self-supporting zeolite monolith catalyst can be used in order to
103 overcome certain problems related to a coated monolith system but still keep the benefits of a
104 macroporous monolith. In order to give a clear understanding of the benefits of a structured
105 catalyst for MTO the reaction is briefly discussed. The possible opportunities of structured
106 catalysts in improving the selectivity, activity and stability of the reaction are highlighted. In a
107 second part different structured supports and the coating of these supports is covered followed
108 by examples of coated structured catalysts for MTO. In a final part of this paper the self-
109 supporting structured catalysts are discussed.

110

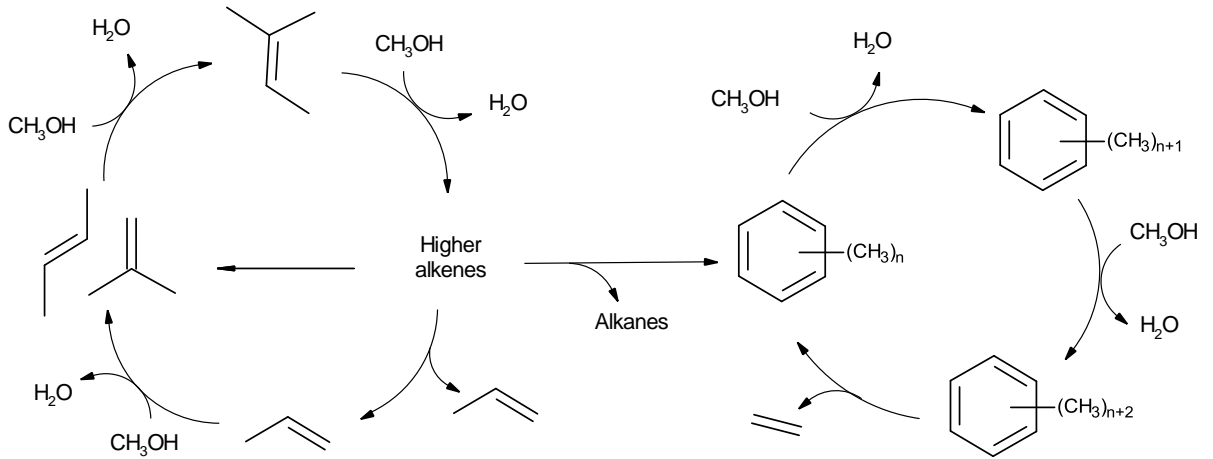
111

Reaction mechanism and selectivity

112

113 Over time several mechanisms have been proposed. Studies of the reaction mechanism
114 by Dahl and Kolboe (Bjorgen et al. 2007; Dahl and S Kolboe 1994; Dahl and Stein Kolboe
115 1993; Mores et al. 2008; Unni Olsbye et al. 2005; S Svelle et al. 2005; Stian Svelle, Rønning,
116 and Stein Kolboe 2004) in SAPO-34 have suggested the hydrocarbon pool mechanism which
117 is now generally accepted (Hemelseot, Van der Mynsbrugge, De Wispelaere, Waroquier, &
118 Van Speybroeck, 2013). In ZSM-5 however, the observations point to a dual cycle
119 mechanism shown in Figure 1, with a hydrocarbon pool mechanism responsible for ethylene
120 formation and a repeated methylation-cracking reaction for the formation of propylene (S
121 Svelle et al., 2005; Stian Svelle et al., 2004). The questions whether both these cycles operate
122 independently of each other is still of great interest to researchers as this has a great influence
123 on the selectivity of the reaction (Olsbye et al., 2012).

124



125
126

127 *Figure 1: Representation of dual cycle mechanism in H-ZSM-5 (after Olsbye et al., 2005).*

128

129 Intrinsic catalyst properties such as strength and density of the acid sites (Aramburo et
 130 al., 2011; Furumoto et al., 2011; Park, Kim, et al., 2008; Tago, Iwakai, Morita, Tanaka, &
 131 Masuda, 2005; Westgård Erichsen, Svelle, & Olsbye, 2013; W. Wu, Guo, Xiao, & Luo, 2011)
 132 and zeolite topology (Hereijgers et al., 2009; Li et al., 2011; Mccann et al., 2008; Ocampo et
 133 al., 2010; Park, Lee, Kim, Hong, & Seo, 2008) have an influence on the selectivity of the
 134 MTO reaction. In the past decade, research has focused on the modification of the acidity of
 135 the catalysts by changing the Si/Al ratio (Ferreira Madeira et al., 2012; Inoue, Okabe, Inaba,
 136 Takahara, & Murata, 2010), by incorporation of metal or phosphor in the zeolite (Kaarsholm
 137 et al., 2007; Rahimi & Karimzadeh, 2011; Takahashi, Xia, Nakamura, Shimada, & Fujitani,
 138 2012; Valle, Alonso, Atutxa, Gayubo, & Bilbao, 2005; Y. Yang et al., 2012) or via
 139 modification by a binder (Yun-Jo Lee, Kim, Viswanadham, Jun, & Bae, 2010; Menges &
 140 Kraushaar-Czarnetzki, 2012). It was observed that lower acid site density, especially lower
 141 strong acid site density results in better selectivity and stability due to sparse distribution of
 142 alkylaromatics in the pores, suppressing the coke formation. The effect of reaction conditions
 143 (Taheri Najafabadi, Fatemi, Sohrabi, & Salmasi, 2012) and feed composition (X. Wu &
 144 Anthony, 2001) on the selectivity has also been explored. The most important reaction
 145 parameters influencing the selectivity and stability of the reaction are the temperature, the
 146 methanol space-time and the inlet water-methanol ratio. The co-addition of water to the
 147 reaction mixture has a double effect: it both influences the selectivity by shifting the methanol
 148 dehydration equilibrium and decreases the deactivation by coking by blocking the strongest
 149 acid sites.

150

151 The selectivity is also influenced by the diffusion properties of the catalyst, such as the
152 crystal size of the zeolite (Bleken et al., 2012; De Chen, Moljord, Fuglerud, & Holmen, 1999;
153 Dahl et al., 1999; Meng, Mao, Guo, & Lu, 2012; Möller & Böhringer, 1999; Rownaghi,
154 Rezaei, & Hedlund, 2011). Modeling and catalytic experiments have shown that the diffusion
155 is altered by the macroscopic properties of the catalyst structure, which has its consequences
156 for the selectivity, activity and stability of the catalyst (Guo, Wu, Luo, & Xiao, 2012; Zhuang,
157 Gao, Zhu, & Luo, 2012). The reaction mechanism suggest that fast evacuation of the reaction
158 products from the catalyst is needed as further reaction of products such as propylene and
159 butylene is possible. Kinetic studies performed by Svelle et al. have shown the importance of
160 the contact time (S Svelle et al., 2005; Stian Svelle et al., 2004). It was shown that long
161 contact times led to an increased yield of aromatics and alkanes whereas by fast evacuation of
162 the alkene products, the formation of aromatics can be reduced and high $C_3^=/C_2^=$ ratios can be
163 achieved. Moreover, the fast evacuation of products can reduce the coke formation on the
164 zeolite surface thus increasing the stability. To control the residence time, contact time and
165 kinetics of molecules in a chemical reaction three factors are crucial: the residence time in the
166 zeolite micropores, in the catalyst bulk phase and in the gas phase of the reactor. By using a
167 structured catalyst, all three time components can be modified independently. To do so, the
168 zeolite crystal size, the thickness and porosity of the zeolite coating, and the architecture of
169 the macroporous structure can be altered respectively. By modification of these three
170 variables, the yield of valuable products of the MTO reaction can be improved and optimized.

171

172

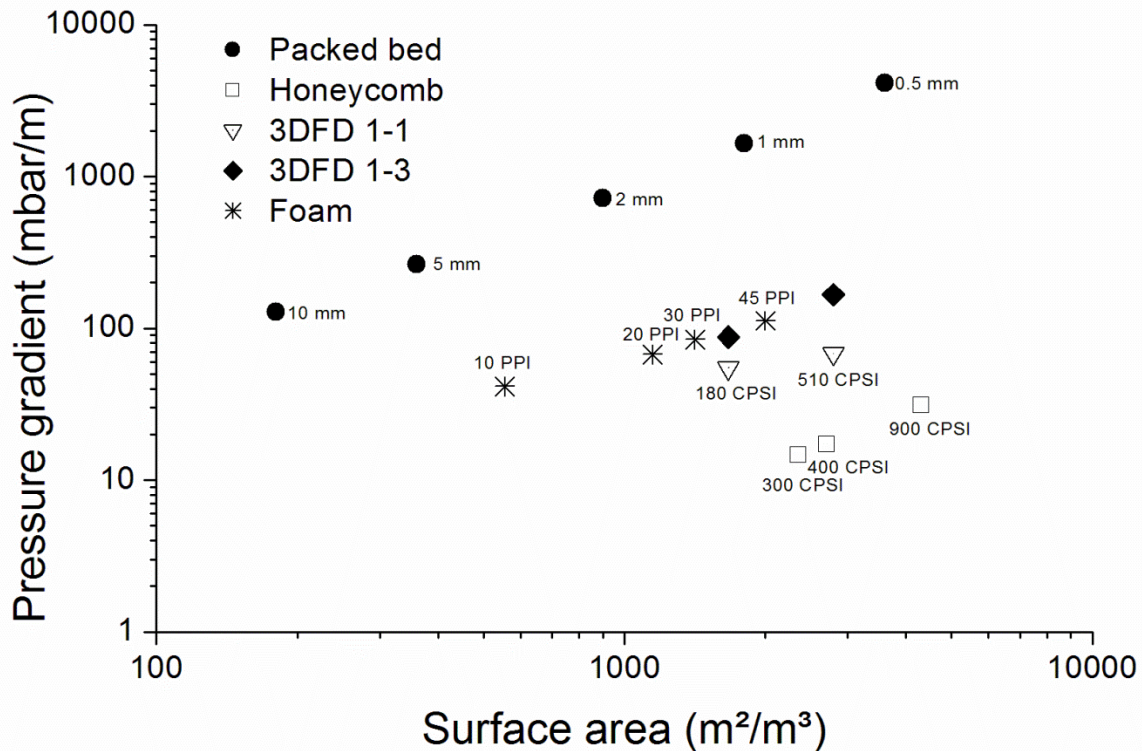
Structured catalysts

173

174 Catalysts in industrial applications are generally shaped as pellets, micro granules or
175 extrudates and used in a random packed bed. Fast evacuation of the products can be achieved
176 by applying zeolites with small crystal sizes and introducing good mass transfer properties in
177 the catalyst and/or catalytic bed. The mass transfer in a reactor with a packed bed of zeolite
178 pellets can be improved by reducing the size of the zeolites pellets. However, this will lead to
179 a higher pressure drop over the reactor and can lead to a serious operating cost in industrial
180 installations. This high pressure drop can be avoided by using hierarchical porous catalysts,
181 either by applying a macroporous support coated with the catalyst or by introduction of meso-
182 and macropores in the zeolite particle. Mitchell et al. have shown that the stability of a
183 hierarchical ZSM-5 is significantly higher than a conventional ZSM-5 catalyst for the MTO

184 reaction in a packed bed (Mitchell, Michels, Kunze, & Pérez-Ramírez, 2012; Mitchell,
185 Michels, & Pérez-Ramírez, 2013). In this way, high mass transfer can be achieved without
186 the high pressure drop penalty, additionally the stability of the zeolite can be increased (Guo,
187 Wu, et al., 2012). The architecture of the structured catalysts has an impact on the residence
188 time distribution of the molecules and thus the selectivity. A well designed structured catalyst
189 can improve the selectivity and the stability of the catalyst system by achieving a narrower
190 residence time distribution (Pangarkar et al., 2008). Structured catalysts are therefore a
191 promising alternative as they allow a low pressure drop in combination with high mass- and
192 heat transfer and controlled residence times (Dai, Lei, Li, & Chen, 2012; Lefevre, Gysen,
193 Mullens, Meynen, & Van Noyen, 2013). In Figure 2 the pressure drop of different honeycomb
194 monolith structures is compared to packed beds of spheres and rings. It is shown that the
195 pressure drop increases with smaller particles or smaller channels. At the same specific
196 surface area the samples show different pressure drop, respectively from high to low: spheres
197 (packed bed), foams \approx 3DFD 1-3, 3DFD 1-1 and honeycombs. The void fraction of a packed
198 bed of spheres is low (40 %) as compared to the structured packings were the macroporous
199 architecture results in a void fraction of 70-80 %. The results shown in figure 3 indicate a
200 large influence of the porous architecture on the pressure drop of the structured packing.

201



202

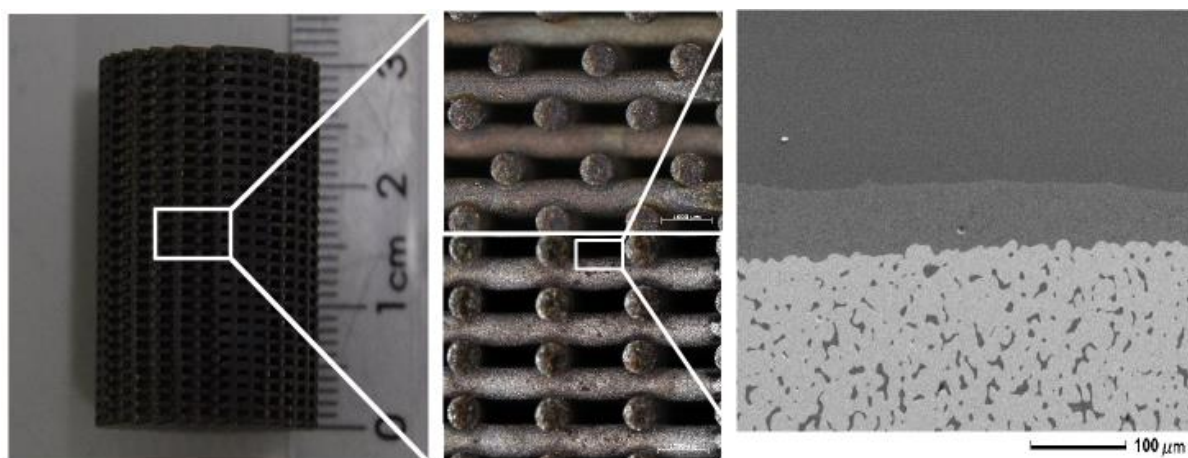
203 Figure 2: Pressure drop as function of specific geometric surface area of foams, honeycombs, 3DFD
 204 structures and spheres. Data are for air at 20 °C and 1 bar and a superficial gas velocity of 2.5 m/s (at
 205 STP) (CPSI: cells per square inch; PPI: Pores per inch) (Dietrich, 2012).

206

207 Many types of structured support materials have been proposed in literature.
 208 Conventional structured packings can be subdivided in four different classes: (1) ceramic or
 209 metallic monoliths with straight parallel channels, (2) sheet/gauze metallic packings, (3)
 210 knitted metallic wire packings and (4) open cell ceramic or metallic foams. The type of
 211 support material will have an impact on the mass and heat transfer properties, the pressure
 212 drop and the catalyst hold up. Alternatively, a new type of structured packing with high
 213 flexibility of the porous architecture was proposed. Recently the use of 3D-printing or 3
 214 dimensional fiber deposition (3DFD) for manufacturing catalyst support structures has been
 215 proposed. This flexible technique allows optimization of the architecture of the support
 216 combining good mass and heat transfer properties with low pressure drop (Ferrizz, Stuecker,
 217 Cesarano III, & Miller, 2005; Lefevre et al., 2013; Lewis, Smay, Stuecker, & Cesarano,
 218 2006; Stuecker, Miller, Ferrizz, Mudd, & Cesarano, 2004; Van Noyen, Wilde, Schroeven,
 219 Mullens, & Luyten, 2012). By constructing the catalyst support material layer by layer there
 220 is large freedom of design of the architecture of the support (Figure 3). The thickness of the

221 fibers, the distance between the fibers, the stacking of the fibers can be varied and
222 manufactured in different materials such as stainless steel, cordierite or titania. The stacking
223 of the fibers will have a major impact on the mass and heat transfer properties and pressure
224 drop of the final catalyst (Ferrizz et al., 2005; Stuecker et al., 2004). The flexibility of the
225 3DFD technology allows to specifically enhance properties of the structured packing allowing
226 research on the impact of these properties of the architecture of the support material for
227 different types of reactions (Leong, Cheah, & Chua, 2003). Rapid prototyping of ceramic and
228 metallic supports allows an almost unlimited amount of unique architectures with an excellent
229 reproducibility. By combination of modeling and testing, a fast and good choice of supports
230 with adequate mechanical properties and low pressure drop can be achieved (Van Noyen et
231 al., 2012).

232



233

234 *Figure 3:* Different scales of 3DFD support structure respectively: full scale structure, different
235 stacking of the layers of the 3DFD structure (1-3 on top and 1-1 on the bottom) and ZSM-5 coating on
236 the 3DFD surface.

237

238 The straight channels of standard cordierite honeycombs have some disadvantages like
239 problems with the bulk gas-solid mass transfer and problems with heat transfer in exothermal
240 reactions such as MTO which can lead to hot spots. These problems can be overcome by
241 different types of materials like foams or 3D ordered structures or metallic honeycombs with
242 higher heat conductivity (Pangarkar et al., 2008). These structures promote turbulent flow and
243 allow inter channel diffusion leading to better mass and heat transfer (Ferrizz et al., 2005;
244 Stuecker et al., 2004). Structures with a predetermined 3D porous network are of great interest
245 as these are highly reproducible and the ideal flow pattern in the structure can be chosen in

246 advance. In Table 1 an overview is given of the different properties of the classes of
247 structured packings.

248

<i>Parameter</i>	<i>Packed bed</i>	<i>Ceramic/ metallic monolith</i>	<i>Sheet/gauze metallic packing</i>	<i>Knitted wire packing</i>	<i>Foam</i>	<i>3DFD</i>
Radial mass transfer	medium	no	good	no data	good	good
Radial heat transfer	medium	no	good	no data	good	good
Tortuosity of fluid	yes	no	yes	yes	yes	yes
Pressure drop	high	low	low	low	low	low
Geometric macroporosity	low	high	high	high	high	high
Price	low	low	medium	medium-low	medium-low	medium- high
Flexibility	low	low	medium	low	low	high

249 **Table 1:** Properties of conventional structured packings and 3DFD structured packings.(Pangarkar et
250 al., 2008)

251

252 To obtain the active catalyst, coatings of zeolite particles are deposited on the inert
253 structured surface (Ulla et al., 2003). There are two main techniques used to deposit a coating
254 of the active zeolite on the surface of the support: wash coating (Zhu, Fan, & Xu, 2011) and
255 hydrothermal coating (Ivanova et al., 2009; Louis, Ocampo, Yun, Tessonier, & Pereira,
256 2010; Perdana, Creaser, Lindmark, & Hedlund, 2010; Seijger & Oudshoorn, 2000; Shan &
257 Kooten, 2000; H. Yang, Liu, Gao, & Xie, 2010; Yao, Zeng, Zhang, & Xu, 2008; Zampieri et
258 al., 2006). The most important differences between wash coatings and hydrothermal coatings
259 are the presence or absence of intra crystalline porosity, the bonding strength of the zeolites to
260 the support, the thickness of the coating and the uniformity of the coating (Table 2) (Seijger &
261 Oudshoorn, 2000; J. M. Zamaro & Miró, 2010).

262

<i>Method</i>	<i>Intra crystalline porosity</i>	<i>Bonding strength</i>	<i>Thickness coating</i>	<i>Uniformity coating</i>
Wash coating	+	-	+	+
Hydrothermal coating	-	+	-	-

263 **Table 2:** Differences between properties of the coated zeolites layer when using wash or hydrothermal
264 coating.

265

266 Although hydrothermal coatings result in high bounding strengths, they also suffer
267 some drawbacks such as tendency for crystallization in the liquid rather than on the surface of
268 the support. The most important variables in selectivity between zeolite deposited on the
269 support and in the coating solution are (i) decreasing the ratio of the synthesis mixture volume
270 to the packing surface area (ii) agitating the synthesis solution during synthesis (iii) lowering

271 the amount of reagent concentration of the synthesis mixture (iv) increasing the template
272 concentration near the support surface and (v) creating a seeding surface on the support
273 surface (Seijger & Oudshoorn, 2000; Shan & Kooten, 2000). Moreover, the loading of zeolite
274 on the support using hydrothermal synthesis is limited in a single coating step. Prolonged
275 synthesis time initially leads to an increase in loading but this effect decreases with increasing
276 time. By repeated hydrothermal coating steps with a fresh synthesis solution on the same
277 carrier, the loading increases proportionally with the number of coatings. Not only the
278 thickness of the layer increases but also the density and the crystal size of the layer, as the first
279 layer acts as a seeding for further coatings (Shan & Kooten, 2000; Van Noyen et al., 2012). It
280 should be noted that the Si/Al ratio changes with repeated coatings, which has a direct impact
281 on the acidity and the catalytic properties of the zeolite layer (Shan & Kooten, 2000). Another
282 issue with hydrothermal coating is the high density of the coated layer, as a porous layer is
283 beneficial for good mass transfer inside the zeolite coating (S. Lopez-Orozco, A. Inayat, A.
284 Schwab, 2011).

285

286 On the other hand, the adhesion of zeolite wash coatings to the support structure is
287 often an issue. Additional inorganic binders can be used in low concentration to improve the
288 adhesion of the zeolite to the surface of the support (Buciuman & Kraushaar-Czarnetzki,
289 2001). However, the binder can inhibit the diffusion of reactants and products in the coating
290 as it is usually smaller than the zeolite particles, possibly blocking the entrance of the pores of
291 the zeolite. Buciuman & Kraushaar-Czarnetzki showed it was possible to wash coat ZSM-5
292 and silicalite-1 directly onto a foam without the use of additives (Buciuman & Kraushaar-
293 Czarnetzki, 2001). Uniform zeolite coatings were obtained for different carriers at a
294 suspension zeolite concentration of 0.1-10 wt%. By increasing the zeolite concentration of the
295 dipping suspension higher loadings on the foam could be achieved. The adhesion strength of
296 the coating was tested using high air flow. A weight loss of about 10% of the zeolite loading
297 was observed after 48h in a 1 m/s air flow, which is still too high for industrial applications.
298 Another more demanding test for the adhesion of the coating is the use of ultrasonic
299 conditions. By optimization of the particle size and the addition of binders a stable coating of
300 ZSM-5 on cordierite honeycomb can be obtained as shown by Zamaro et al. and Lefevre et
301 al. (Lefevre et al., 2013; J. Zamaro, Ulla, & Miro, 2005).

302

303 ZSM-5 is commonly used as catalyst in structured supports for methanol-to-olefins,
304 because the deactivation by coking is too fast for SAPO-34 (Bleken et al., 2012). ZSM-5

305 coatings have been deposited on different types of support materials such as stainless steel
306 (Shan & Kooten, 2000; H. Yang et al., 2010), Al₂O₃ (Seijger & Oudshoorn, 2000), glass
307 (Louis et al., 2010), ceramic (Ivanova et al., 2009), cordierite (Perdana et al., 2010; Yao et al.,
308 2008; J. Zamaro et al., 2005) or SiC (Ivanova, Louis, Madani, Tessonnier, & Ledoux, 2007;
309 Jiao, Jiang, Yang, & Zhang, 2012; Zampieri et al., 2006). The architecture of the support as
310 well as thickness of the coating and crystal size of the zeolite are of crucial importance for the
311 mass- and heat transfer, pressure drop and contact time during the reaction. Combined with
312 the intrinsic properties of the zeolite used they determine the selectivity and stability of the
313 catalyst. Patcas (Patcas, 2005) has shown that a thick coating layer leads to low catalyst
314 effectiveness and low olefin yield. On the other hand, when applying a very thin layer of
315 catalyst it is difficult to keep the catalytic species confined in the micropores. This leads to a
316 too fast evacuation of the reaction species and thus lowers the production of dimethylether,
317 resulting in a low selectivity to light olefins. In conclusion a certain minimum amount/critical
318 thickness of the catalyst coating is needed, although thick coatings should be avoided.

319

320

MTO with structured catalyst

321

322 In Table 3 some examples of catalytic results of ZSM-5 coated structured catalysts for the
323 MTO reaction are given and are compared with a packed bed at the same conditions. Initial
324 work performed by Patcas (2005) shows the better effectiveness of the coated structured
325 catalyst. The use of the coated foam catalyst resulted in a 2.5 times higher production of light
326 olefins per volume of reactor as compared to a packed bed. The results also suggest that the
327 highest light olefin selectivity at 380 °C is achieved at 90 % conversion. Ivanova et al. (2007)
328 have shown that the thickness of the coated layer is an important factor determining the
329 selectivity. The use of thin coatings results in a fast evacuation of the products and a high
330 selectivity to light olefins. On the other hand, conversion seems to be lower when thin
331 coatings are applied. Although the catalyst hold up per reactor volume is lower using coated
332 structured packings, these types of catalyst can be industrially relevant as the catalyst layer is
333 more effective than in a packed bed. This was shown by Jiao et al. (2012), by comparing a
334 coated foam with a diluted and undiluted packed bed at equal methanol feed per reactor
335 volume. The packed bed of pellets diluted with quartz sand operating at the same WHSV as
336 the coated catalyst showed initially the same selectivity as the composite however, the
337 selectivity and conversion decreased rapidly with time on stream (TOS). On the other hand
338 the undiluted packed bed of pellets working at lower WHSV showed comparable stability and

339 activity as the coated foam but showed significant lower selectivity to propylene. Due to
 340 enhanced mass- and heat transfer properties of the structured catalyst better catalytic results
 341 are achieved with less catalyst. These results were confirmed in the work of Bleken et al.
 342 (2012) where the propylene yield of zeolite coated glass monolith was higher than that for the
 343 packed bed. Moreover, at the same WHSV the reference zeolite particles showed faster
 344 deactivation than the coated sample. Lefevre et al. (2013) have shown that the importance of
 345 the architecture and material of the support structure on the performance of the final catalyst.
 346 The 3DFD 1-3 structure, with zigzag channels in the direction of the flow, shows the best
 347 yield of light olefins. Interestingly, the 3DFD 1-1 with straight channels shows higher
 348 selectivity than the honeycomb structure with straight channels and the same loading. This
 349 could be a result of the higher thermal conductivity of the steel support or the radial channels
 350 of the 3DFD support allowing radial mass- and heat transfer. The importance of porosity in
 351 the coated layer was highlighted by Jiao et al. (2013). A conventional hydrothermal coated
 352 structure was compared to a sample coated using a two-step coating. The second method
 353 resulted in a zeolite layer with high porosity at the surface of the layer and a denser zeolite
 354 layer at the surface of the support. This gradient coating combines the good adherence of the
 355 coating to the support with excellent accessibility of the zeolite. The catalytic results show
 356 that the improved mass transfer properties in the gradient sample result in higher propylene
 357 selectivity and longer stability than the conventional sample.

358

<i>Catalyst structure</i>	<i>Temp</i> <i>. (°C)</i>	<i>WHSV</i> <i>(h⁻¹)</i>	<i>Conv.</i> <i>(%)</i>	<i>C₂H₄</i> <i>(%)</i>	<i>C₃H₆</i> <i>(%)</i>	<i>C₄H₈</i> <i>(%)</i>	<i>Stability</i> <i>(h)</i>	<i>Ref.</i>
5 μm coating α-alumina foam	380	27	90	34	-	-	-	(Patcas, 2005)
18 μm coating α-alumina foam	380	40	90	32	-	-	-	(Patcas, 2005)
Packed bed	380	8	90	22	-	-	-	(Patcas, 2005)
Single coated SiC foam	500	-	76	-	C ₂ ⁼ -C ₄ ⁼ : 65	-	8	(Ivanova et al., 2007)
Double coated SiC foam	500	-	90	-	C ₂ ⁼ -C ₄ ⁼ : 60	-	10	(Ivanova et al., 2007)
Packed bed	500	-	70	-	C ₂ ⁼ -C ₄ ⁼ : 55	-	12	(Ivanova et al., 2007)
ZSM-5 coated SiC foam	500	4.46	100	-	37	-	50+	(Jiao et al., 2012)
Packed bed ZSM-5 diluted	500	4.46	95	-	30	-	35	(Jiao et al., 2012)

Packed bed ZSM-5 undiluted	500	0.75	100	-	25	-	50+	(Jiao et al., 2012)
ZSM-5 Packed bed	350	1.8	99	15	27	14	-	(Bleken et al., 2012)
ZSM-5 coating on glass monolith	350	1.8	99	12	30	18	-	(Bleken et al., 2012)
Coated cordierite honeycomb	350	18	99.7	C ₂ ⁼ -C ₃ ⁼ : 41.1		-	-	(Lefevere et al., 2013)
Coated stainless steel 3DFD straight channels	350	18	87.6	C ₂ ⁼ -C ₃ ⁼ : 65.8		-	-	(Lefevere et al., 2013)
Coated stainless steel 3DFD zigzag channels	350	18	98.9	C ₂ ⁼ -C ₃ ⁼ : 55.5		-	-	(Lefevere et al., 2013)
Packed bed SiC foam conventional	350	4.5	84.6	C ₂ ⁼ -C ₃ ⁼ : 48.7		-	-	(Lefevere et al., 2013)
ZSM-5 coating SiC foam gradient	500	0.6	97.5	8.2	37.8	19.9	-	(Jiao et al., 2013)
ZSM-5 coating	500	0.6	99.5	7.1	45.1	24.6	-	(Jiao et al., 2013)

359 *Table 3: Overview of catalytic results for the MTO reaction using zeolite coated monolith catalysts.*

360

361

Bulk monolithic catalyst

362 Monoliths with the catalyst incorporated in the structure, so called ‘bulk monolithic catalysts’
 363 offer some advantages over the coated monolithic structures. First of all it is clear that
 364 synthesis of a coated catalyst needs more process steps than preparation of a bulk monolithic
 365 catalyst. For coated structures repeated coatings are often needed in order to obtain the
 366 necessary catalyst loading, this can lead to non-uniformity of the coating. Non-uniformity of
 367 the coating affects the mechanical properties as well as the mass- and heat transfer of the final
 368 catalyst. One of the most important drawbacks of a coated catalyst is the limited loading of
 369 catalyst per reactor volume. Using a bulk monolithic catalyst these shortcomings are
 370 overcome, a high amount of catalyst can be uniformly introduced in the reactor (Zamaniyan,
 371 Mortazavi, Khodadadi, & Manafi, 2010).

372

373 Modeling studies by Guo et al. (Guo, Wu, et al., 2012; Guo, Xiao, & Luo, 2012) have shown
 374 that a major improvement of the mass transfer properties is made by using a self-supporting

375 zeolite honeycomb over a randomly packed bed of particles. By using the zeolite ZSM-5
 376 honeycomb it was calculated that the efficiency of the catalyst in the reactor went up five
 377 times, so lower space times were needed to obtain the higher conversion. Moreover, the
 378 selectivity to propylene was raised by using the honeycomb structure. It was found that the
 379 wall thickness of the monolith affects the product distribution, especially of C₃-C₆ alkanes. It
 380 was suggested that monoliths with high cell density and thin walls achieved the highest
 381 propylene yield, a zeolitic honeycomb structure with 400 cells per square inch and 200 μm
 382 was proposed.

383

384 Some work has already been done on the formation of ZSM-5 self-supporting monolith
 385 structures. Aranzabal et al. (Aranzabal et al., 2010) have optimized direct extrusion of ZSM-5
 386 zeolite paste into a honeycomb shape. A series of process steps (kneading, extruding, drying,
 387 calcination) are crucial to obtain a highly stable defect-free structure. Good rheology of the
 388 paste is needed in order to ensure successful extrusion. Good mechanical properties are
 389 obtained using a colloidal silica binder in a concentration of 10-25 wt% of the final catalyst.
 390 An alternative method for the synthesis of a self-supporting ZSM-5 monolith is the use of a
 391 template. In this method a hydrothermal synthesis of zeolite on the template surface is
 392 performed, afterwards the template is removed in order to leave a macroporous self-
 393 supporting monolith. The use of polyurethane foam in order to synthesize a ZSM-5 self-
 394 supporting foam was proposed by Lee et al. (Y.-J. Lee, Lee, Park, & Yoon, 2001; Yun-Jo
 395 Lee et al., 2009). Foams with three different Si/Al ratios were synthesized, their catalytic
 396 properties were compared for conversion of methanol to light olefins. As reference material
 397 the foam with the best performance (Si/Al = 250) was pelletized and compared with the
 398 monolithic structure. The catalytic results at 450°C (Table 4) show that the monoliths have
 399 good selectivity to light olefins however the selectivity is only slightly higher than that of the
 400 packed bed. The main difference between the ZSM-5 foam and the pelletized zeolite is
 401 revealed in the testing of the conversion at higher WHSV. The monolith shows superior
 402 activity at high WHSV confirming the better efficiency of a structured self-supporting
 403 catalyst. Overall, the results of the modeling studies in combination with the catalytic study
 404 show promising opportunities for self-supporting ZSM-5 structures in the methanol-to-olefins
 405 reaction especially if high propylene selectivity is desired.

406

<i>Catalyst structure</i>	<i>Temp.</i> (°C)	<i>WHSV</i> (h ⁻¹)	<i>Conv.</i> (%)	<i>C₂H₄</i> (%)	<i>C₃H₆</i> (%)	<i>C₄H₈</i> (%)	<i>Stability</i> (h)	<i>Ref.</i>
---------------------------	----------------------	-----------------------------------	---------------------	--	--	--	-------------------------	-------------

ZSM-5 foam (Si/Al= 140)	450	2.55	100	11.0	28.6	19.5	-	(Yun-Jo Lee et al., 2009)
ZSM-5 foam (Si/Al= 250)	450	2.55	100	11.4	43.9	20.1	-	(Yun-Jo Lee et al., 2009)
ZSM-5 foam (Si/Al= 500)	450	2.55	75.5	5.4	39.6	20.2	-	(Yun-Jo Lee et al., 2009)
Packed bed pelletized ZSM-5 (Si/Al= 250)	450	2.55	100	10.4	41.5	20.8	-	(Yun-Jo Lee et al., 2009)

407 *Table 4: Overview of catalytic results for the MTO reaction using self-supporting zeolite monolith*
 408 *catalysts.*

409

410

410 Conclusions

411

412 The reaction mechanism of the MTO process has shown that next to the intrinsic
 413 properties of the zeolite also the crystal size of the zeolite, the porous architecture of the
 414 catalyst are important. Fast removal of the products and heat of the MTO reaction and
 415 narrower contact time distribution can be achieved by using structured macroporous catalyst
 416 systems. The catalytic results of different research groups have shown that higher selectivity
 417 towards propylene and longer stability of the catalyst can be achieved. The higher mass- and
 418 heat transfer properties of these hierarchical materials lead to faster evacuation of the desired
 419 products. Moreover, the results of the coated systems point out the higher effectiveness of the
 420 catalyst layer and in this way overcoming the lower amount of catalyst per volume of these
 421 systems. On the other hand, the self-supporting zeolite monoliths offer an alternative to raise
 422 the loading of zeolite per reactor volume and reducing the number of manufacturing steps of
 423 the catalyst. Combining the high selectivity and stability of the structured catalysts and high
 424 loading of catalyst per reactor volume these self-supporting monoliths offer a promising route
 425 for process intensification.

426

In future work, the optimization of the architecture of the macroporous material can
 427 lead to further improvement of the stability and selectivity of the catalyst. 3D printing of the
 428 support using 3DFD technology can be an interesting tool to investigate the effect of
 429 architecture as it allows a high freedom of design of the catalyst structure. In combination
 430 with modeling studies faster optimization of the architecture of the support with the 3DFD
 431 technology can be achieved, which can lead to optimization of the propylene yield of the
 432 catalyst.

433

References

- 435 Aramburo, L. R., Karwacki, L., Cubillas, P., Asahina, S., de Winter, D. a M., Drury, M. R.,
436 ... Weckhuysen, B. M. (2011). The porosity, acidity, and reactivity of dealuminated
437 zeolite ZSM-5 at the single particle level: the influence of the zeolite architecture.
438 *Chemistry a European Journal*, 17(49), 13773–81. doi:10.1002/chem.201101361
- 439 Aranzabal, A., Iturbe, D., Romero-Sáez, M., González-Marcos, M. P., González-Velasco, J.
440 R., & González-Marcos, J. a. (2010). Optimization of process parameters on the
441 extrusion of honeycomb shaped monolith of H-ZSM-5 zeolite. *Chemical Engineering*
442 *Journal*, 162(1), 415–423. doi:10.1016/j.cej.2010.05.043
- 443 Bjorgen, M., Svelle, S., Joensen, F., Nerlov, J., Kolboe, S., Bonino, F., ... Olsbye, U. (2007).
444 Conversion of methanol to hydrocarbons over zeolite H-ZSM-5: On the origin of the
445 olefinic species. *Journal of Catalysis*, 249(2), 195–207. doi:10.1016/j.jcat.2007.04.006
- 446 Bleken, F. L., Chavan, S., Olsbye, U., Boltz, M., Ocampo, F., & Louis, B. (2012). Conversion
447 of methanol into light olefins over ZSM-5 zeolite: Strategy to enhance propene
448 selectivity. *Applied Catalysis A: General*, 447-448, 178–185.
449 doi:10.1016/j.apcata.2012.09.025
- 450 Buciuman, F., & Kraushaar-Czarnetzki, B. (2001). Preparation and characterization of
451 ceramic foam supported nanocrystalline zeolite catalysts. *Catalysis today*, 69, 337–342.
452 doi:10.1016/S0920-5861(01)00387-X
- 453 Chae, H.-J., Song, Y.-H., Jeong, K.-E., Kim, C.-U., & Jeong, S.-Y. (2010). Physicochemical
454 characteristics of ZSM-5/SAPO-34 composite catalyst for MTO reaction. *Journal of*
455 *Physics and Chemistry of Solids*, 71(4), 600–603. doi:10.1016/j.jpcs.2009.12.046
- 456 Chen, D., Moljord, K., & Holmen, a. (2012). A methanol to olefins review: Diffusion, coke
457 formation and deactivation on SAPO type catalysts. *Microporous and Mesoporous*
458 *Materials*, 164, 239–250. doi:10.1016/j.micromeso.2012.06.046
- 459 Chen, De, Moljord, K., Fuglerud, T., & Holmen, A. (1999). The effect of crystal size of
460 SAPO-34 on the selectivity and deactivation of the MTO reaction. *Microporous and*
461 *Mesoporous Materials*, 29(1-2), 191–203. doi:10.1016/S1387-1811(98)00331-X
- 462 Chen, J. Q., Bozzano, A., Glover, B., Fuglerud, T., & Kvisle, S. (2005). Recent advancements
463 in ethylene and propylene production using the UOP/Hydro MTO process. *Catalysis*
464 *Today*, 106(1-4), 103–107. doi:10.1016/j.cattod.2005.07.178
- 465 Dahl, I. M., & Kolboe, S. (1993). On the reaction mechanism for propene formation in the
466 MTO reaction over SAPO-34. *Catalysis Letters*, 20(3-4), 329–336.
467 doi:10.1007/BF00769305
- 468 Dahl, I. M., & Kolboe, S. (1994). On the reaction mechanism for hydrocarbon formation from
469 Methanol over SAPO-34 1 isotopic labeling studies. *Journal of Catalysis*, 149, 458–464.
470 doi:10.1006/jcat.1996.0188

- 471 Dahl, I. M., Wendelbo, R., Andersen, A., Akporiaye, D., Mostad, H., & Fuglerud, T. (1999).
472 The effect of crystallite size on the activity and selectivity of the reaction of ethanol and
473 2-propanol over SAPO-34. *Microporous and Mesoporous Materials*, 29(1-2), 159–171.
474 doi:10.1016/S1387-1811(98)00328-X
- 475 Dai, C., Lei, Z., Li, Q., & Chen, B. (2012). Pressure drop and mass transfer study in
476 structured catalytic packings. *Separation and Purification Technology*, 98, 78–87.
477 doi:10.1016/j.seppur.2012.06.035
- 478 Dietrich, B. (2012). Pressure drop correlation for ceramic and metal sponges. *Chemical*
479 *Engineering Science*, 74, 192–199. doi:10.1016/j.ces.2012.02.047
- 480 Ferreira Madeira, F., Ben Tayeb, K., Pinard, L., Vezin, H., Maury, S., & Cadran, N. (2012).
481 Ethanol transformation into hydrocarbons on ZSM-5 zeolites: Influence of Si/Al ratio on
482 catalytic performances and deactivation rate. Study of the radical species role. *Applied*
483 *Catalysis A: General*, 443-444, 171–180. doi:10.1016/j.apcata.2012.07.037
- 484 Ferrizz, R., Stuecker, J., Cesarano III, J., & Miller, J. (2005). Monolithic supports with unique
485 geometries and enhanced mass transfer. *Ind. & Eng. Chem. Res.*, 44(2), 302–308.
486 doi:10.1021/ie049468r
- 487 Furumoto, Y., Harada, Y., Tsunoji, N., Takahashi, A., Fujitani, T., Ide, Y., ... Sano, T.
488 (2011). Effect of acidity of ZSM-5 zeolite on conversion of ethanol to propylene.
489 *Applied Catalysis A: General*, 399(1-2), 262–267. doi:10.1016/j.apcata.2011.04.009
- 490 Guo, W., Wu, W., Luo, M., & Xiao, W. (2012). Modeling of diffusion and reaction in
491 monolithic catalysts for the methanol-to-propylene process. *Fuel Processing Technology*,
492 6–11. doi:10.1016/j.fuproc.2012.06.005
- 493 Guo, W., Xiao, W., & Luo, M. (2012). Comparison among monolithic and randomly packed
494 reactors for the methanol-to-propylene process. *Chemical Engineering Journal*, 207-208,
495 734–745. doi:10.1016/j.cej.2012.07.046
- 496 Hemelsoet, K., Van der Mynsbrugge, J., De Wispelaere, K., Waroquier, M., & Van
497 Speybroeck, V. (2013). Unraveling the reaction mechanisms governing methanol-to-
498 olefins catalysis by theory and experiment. *Chemphyschem : a European journal of*
499 *chemical physics and physical chemistry*, 14, 1526–45. doi:10.1002/cphc.201201023
- 500 Hereijgers, B. P. C., Bleken, F., Nilsen, M. H., Svelle, S., Lillerud, K.-P., Bjørgen, M., ...
501 Olsbye, U. (2009). Product shape selectivity dominates the Methanol-to-Olefins (MTO)
502 reaction over H-SAPO-34 catalysts. *Journal of Catalysis*, 264(1), 77–87.
503 doi:10.1016/j.jcat.2009.03.009
- 504 Inoue, K., Okabe, K., Inaba, M., Takahara, I., & Murata, K. (2010). Metal modification
505 effects on ethanol conversion to propylene by H-ZSM-5 with Si/Al₂ ratio of 150.
506 *Reaction Kinetics, Mechanisms and Catalysis*, 101(2), 477–489. doi:10.1007/s11144-
507 010-0245-4

- 508 Ivanova, S., Louis, B., Madani, B., Tessonnier, J. P., & Ledoux, M. J. (2007). ZSM-5
509 Coatings on -SiC Monoliths : Possible New Structured Catalyst for the Methanol-to-
510 Olefins Process. *J. Phys. Chem. C*, *111*, 4368–4374. doi:10.1021/jp067535k
- 511 Ivanova, S., Vanhaecke, E., Dreibine, L., Louis, B., Pham, C., & Pham-huu, C. (2009).
512 General Binderless HZSM-5 coating on b -SiC for different alcohols dehydration.
513 *Applied Catalysis A: General*, *359*, 151–157. doi:10.1016/j.apcata.2009.02.024
- 514 Jiao, Y., Jiang, C., Yang, Z., Liu, J., & Zhang, J. (2013). Synthesis of highly accessible ZSM-
515 5 coatings on SiC foam support for MTP reaction. *Microporous and Mesoporous*
516 *Materials*, *181*, 201–207. doi:10.1016/j.micromeso.2013.07.013
- 517 Jiao, Y., Jiang, C., Yang, Z., & Zhang, J. (2012). Controllable synthesis of ZSM-5 coatings on
518 SiC foam support for MTP application. *Microporous and Mesoporous Materials*, *162*,
519 152–158. doi:10.1016/j.micromeso.2012.05.034
- 520 Kaarsholm, M., Joensen, F., Nerlov, J., Cenni, R., Chaouki, J., & Patience, G. S. (2007).
521 Phosphorous modified ZSM-5: Deactivation and product distribution for MTO.
522 *Chemical Engineering Science*, *62*(18-20), 5527–5532. doi:10.1016/j.ces.2006.12.076
- 523 Keil, F. J. (1999). Methanol-to-hydrocarbons: process technology. *Microporous and*
524 *Mesoporous Materials*, *29*(1-2), 49–66. doi:10.1016/S1387-1811(98)00320-5
- 525 Lee, Y.-J., Lee, J. S., Park, Y. S., & Yoon, K. B. (2001). Synthesis of Large Monolithic
526 Zeolite Foams with Variable Macropore Architectures. *Advanced Materials*, *13*(16),
527 1259. doi:10.1002/1521-4095(200108)13:16<1259::AID-ADMA1259>3.0.CO;2-U
- 528 Lee, Yun-Jo, Kim, Y.-W., Jun, K.-W., Viswanadham, N., Bae, J. W., & Park, H.-S. (2009).
529 Textural Properties and Catalytic Applications of ZSM-5 Monolith Foam for Methanol
530 Conversion. *Catalysis Letters*, *129*(3-4), 408–415. doi:10.1007/s10562-008-9811-z
- 531 Lee, Yun-Jo, Kim, Y.-W., Viswanadham, N., Jun, K.-W., & Bae, J. W. (2010). Novel
532 aluminophosphate (AlPO) bound ZSM-5 extrudates with improved catalytic properties
533 for methanol to propylene (MTP) reaction. *Applied Catalysis A: General*, *374*(1-2), 18–
534 25. doi:10.1016/j.apcata.2009.11.019
- 535 Lefevre, J., Gysen, M., Mullens, S., Meynen, V., & Van Noyen, J. (2013). The benefit of
536 design of support architectures for zeolite coated structured catalysts for alcohol-to-
537 olefin conversion. *Catalysis Today*, *216*, 18–23. doi:10.1016/j.cattod.2013.05.020
- 538 Leong, K. F., Cheah, C. M., & Chua, C. K. (2003). Solid freeform fabrication of three-
539 dimensional scaffolds for engineering replacement tissues and organs. *Biomaterials*,
540 *24*(13), 2363–2378. doi:10.1016/S0142-9612(03)00030-9
- 541 Lewis, J. a., Smay, J. E., Stuecker, J., & Cesarano, J. (2006). Direct Ink Writing of Three-
542 Dimensional Ceramic Structures. *Journal of the American Ceramic Society*, *89*(12),
543 3599–3609. doi:10.1111/j.1551-2916.2006.01382.x
- 544 Li, J., Wei, Y., Liu, G., Qi, Y., Tian, P., Li, B., ... Liu, Z. (2011). Comparative study of MTO
545 conversion over SAPO-34, H-ZSM-5 and H-ZSM-22: Correlating catalytic performance

- 546 and reaction mechanism to zeolite topology. *Catalysis Today*, 171(1), 221–228.
547 doi:10.1016/j.cattod.2011.02.027
- 548 Louis, B., Ocampo, F., Yun, H. S., Tessonnier, J. P., & Pereira, M. M. (2010). Hierarchical
549 pore ZSM-5 zeolite structures: From micro- to macro-engineering of structured catalysts.
550 *Chemical Engineering Journal*, 161(3), 397–402. doi:10.1016/j.cej.2009.09.041
- 551 McCann, D. M., Lesthaeghe, D., Kletnieks, P. W., Guenther, D. R., Hayman, M. J.,
552 Speybroeck, V. Van, ... Haw, J. F. (2008). A Complete Catalytic Cycle for
553 Supramolecular Methanol-to-Olefins Conversion by Linking Theory with Experiment
554 **, 5179–5182. doi:10.1002/anie.200705453
- 555 McCann, D. M., Lesthaeghe, D., Kletnieks, P. W., Guenther, D. R., Hayman, M. J., Van
556 Speybroeck, V., ... Haw, J. F. (2008). A Complete Catalytic Cycle for Supramolecular
557 Methanol-to-Olefins Conversion by Linking Theory with Experiment. *Angewandte*
558 *Chemie*, 120(28), 5257–5260. doi:10.1002/ange.200705453
- 559 Meng, T., Mao, D., Guo, Q., & Lu, G. (2012). The effect of crystal sizes of HZSM-5 zeolites
560 in ethanol conversion to propylene. *Catalysis Communications*, 21(3), 52–57.
561 doi:10.1016/j.catcom.2012.01.030
- 562 Menges, M., & Kraushaar-Czarnetzki, B. (2012). Kinetics of methanol to olefins over AlPO₄-
563 bound ZSM-5 extrudates in a two-stage unit with dimethyl ether pre-reactor.
564 *Microporous and Mesoporous Materials*. doi:10.1016/j.micromeso.2012.07.012
- 565 Mitchell, S., Michels, N.-L., Kunze, K., & Pérez-Ramírez, J. (2012). Visualisation of
566 hierarchically structured zeolite bodies from macro to nano length scales. *Nature*
567 *chemistry*, 4, 825–831. doi:10.1038/NCHEM.1403
- 568 Mitchell, S., Michels, N.-L., & Pérez-Ramírez, J. (2013). From powder to technical body: the
569 undervalued science of catalyst scale up. *Chemical Society reviews*.
570 doi:10.1039/c3cs60076a
- 571 Möller, K., & Böhringer, W. (1999). The use of a jet loop reactor to study the effect of crystal
572 size and the co-feeding of olefins and water on the conversion of methanol over HZSM-
573 5. *Microporous and ...*, 29, 127–144. doi:http://dx.doi.org/10.1016/S1387-
574 1811(98)00326-6
- 575 Mores, D., Stavitski, E., Kox, M. H. F., Kornatowski, J., Olsbye, U., & Weckhuysen, B. M.
576 (2008). Space- and time-resolved in-situ spectroscopy on the coke formation in
577 molecular sieves: methanol-to-olefin conversion over H-ZSM-5 and H-SAPO-34.
578 *Chemistry a European Journal*, 14(36), 11320–7. doi:10.1002/chem.200801293
- 579 Ocampo, F., Cunha, J. a., de Lima Santos, M. R., Tessonnier, J. P., Pereira, M. M., & Louis,
580 B. (2010). Synthesis of zeolite crystals with unusual morphology: Application in acid
581 catalysis. *Applied Catalysis A: General*, 390(1-2), 102–109.
582 doi:10.1016/j.apcata.2010.09.037

- 583 Olsbye, U., Bjørgen, M., Svelle, S., Lillerud, K.-P., & Kolboe, S. (2005). Mechanistic insight
584 into the methanol-to-hydrocarbons reaction. *Catalysis Today*, *106*(1-4), 108–111.
585 doi:10.1016/j.cattod.2005.07.135
- 586 Olsbye, U., Svelle, S., Bjørgen, M., Beato, P., Janssens, T. V. W., Joensen, F., ... Lillerud, K.
587 P. (2012). Conversion of methanol to hydrocarbons: how zeolite cavity and pore size
588 controls product selectivity. *Angewandte Chemie (International ed. in English)*, *51*(24),
589 5810–31. doi:10.1002/anie.201103657
- 590 Pangarkar, K., Schildhauer, T. J., van Ommen, J. R., Nijenhuis, J., Kapteijn, F., & Moulijn, J.
591 a. (2008). *Structured Packings for Multiphase Catalytic Reactors. Industrial &*
592 *Engineering Chemistry Research* (Vol. 47, pp. 3720–3751). doi:10.1021/ie800067r
- 593 Park, J. W., Kim, S. J., Seo, M., Kim, S. Y., Sugi, Y., & Seo, G. (2008). Product selectivity
594 and catalytic deactivation of MOR zeolites with different acid site densities in methanol-
595 to-olefin (MTO) reactions. *Applied Catalysis A: General*, *349*(1-2), 76–85.
596 doi:10.1016/j.apcata.2008.07.006
- 597 Park, J. W., Lee, J. Y., Kim, K. S., Hong, S. B., & Seo, G. (2008). Effects of cage shape and
598 size of 8-membered ring molecular sieves on their deactivation in methanol-to-olefin
599 (MTO) reactions. *Applied Catalysis A: General*, *339*(1), 36–44.
600 doi:10.1016/j.apcata.2008.01.005
- 601 Patcas, F. (2005). The methanol-to-olefins conversion over zeolite-coated ceramic foams.
602 *Journal of Catalysis*, *231*, 194–200. doi:10.1016/j.jcat.2005.01.016
- 603 Perdana, I., Creaser, D., Lindmark, J., & Hedlund, J. (2010). Influence of NO_x adsorbed
604 species on component permeation through ZSM-5 membranes. *Journal of Membrane*
605 *Science*, *349*(1-2), 83–89. doi:10.1016/j.memsci.2009.11.030
- 606 Rahimi, N., & Karimzadeh, R. (2011). Catalytic cracking of hydrocarbons over modified
607 ZSM-5 zeolites to produce light olefins: A review. *Applied Catalysis A: General*, *398*(1-
608 2), 1–17. doi:10.1016/j.apcata.2011.03.009
- 609 Ren, T, Patel, M., & Blok, K. (2008). Steam cracking and methane to olefins: Energy use,
610 CO₂ emissions and production costs. *Energy*, *33*, 817–833.
611 doi:10.1016/j.energy.2008.01.002
- 612 Ren, Tao, Daniëls, B., Patel, M. K., & Blok, K. (2009). Petrochemicals from oil, natural gas,
613 coal and biomass: Production costs in 2030–2050. *Resources, Conservation and*
614 *Recycling*, *53*(12), 653–663. doi:10.1016/j.resconrec.2009.04.016
- 615 Rownaghi, A. a., Rezaei, F., & Hedlund, J. (2011). Yield of gasoline-range hydrocarbons as a
616 function of uniform ZSM-5 crystal size. *Catalysis Communications*, *14*(1), 37–41.
617 doi:10.1016/j.catcom.2011.07.015
- 618 S. Lopez-Orozco, A. Inayat, A. Schwab, T. S. (2011). Zeolitic Materials with Hierarchical
619 Porous Structures. *Advanced Materials*, *23*, 2602–2615. doi:10.1002/adma.201100462

- 620 Sano, T., Kiyozumi, Y., & Shin, S. (1992). Synthesis of light olefins from methanol using
621 ZSM-5 type zeolite catalysts. *Sekiyu Gakkai Shi*, 35(6), 429–440. Retrieved from
622 <http://cat.inist.fr/?aModele=afficheN&cpsidt=4540858>
- 623 Seijger, G., & Oudshoorn, O. (2000). In situ synthesis of binderless ZSM-5 zeolitic coatings
624 on ceramic foam supports. *Microporous and Mesoporous Materials*, 39, 195–204.
625 doi:10.1016/S1387-1811(00)00196-7
- 626 Shan, Z., & Kooten, W. Van. (2000). Optimization of the preparation of binderless ZSM-5
627 coatings on stainless steel monoliths by in situ hydrothermal synthesis. *Microporous and*
628 *...*, 34, 81–91. doi:10.1016/S1387-1811(99)00161-4
- 629 Stöcker, M. (1999). Methanol-to-hydrocarbons: catalytic materials and their behavior.
630 *Microporous and Mesoporous Materials*, 29, 3–48. doi:10.1016/S1387-1811(98)00319-9
- 631 Stuecker, J. N., Miller, J. E., Ferrizz, R. E., Mudd, J. E., & Cesarano, J. (2004). Advanced
632 Support Structures for Enhanced Catalytic Activity. *Industrial & Engineering Chemistry*
633 *Research*, 43(1), 51–55. doi:10.1021/ie030291v
- 634 Svelle, S., Ronning, P., Olsbye, U., & Kolboe, S. (2005). Kinetic studies of zeolite-catalyzed
635 methylation reactions. Part 2. Co-reaction of [12C]propene or [12C]n-butene and
636 [13C]methanol. *Journal of Catalysis*, 234(2), 385–400. doi:10.1016/j.jcat.2005.06.028
- 637 Svelle, Stian, Rønning, P. O., & Kolboe, S. (2004). Kinetic studies of zeolite-catalyzed
638 methylation reactions1. Coreaction of [12C]ethene and [13C]methanol. *Journal of*
639 *Catalysis*, 224(1), 115–123. doi:10.1016/j.jcat.2004.02.022
- 640 Tago, T., Iwakai, K., Morita, K., Tanaka, K., & Masuda, T. (2005). Control of acid-site
641 location of ZSM-5 zeolite membrane and its application to the MTO reaction. *Catalysis*
642 *Today*, 105(3-4), 662–666. doi:10.1016/j.cattod.2005.06.009
- 643 Taheri Najafabadi, A., Fatemi, S., Sohrabi, M., & Salmasi, M. (2012). Kinetic modeling and
644 optimization of the operating condition of MTO process on SAPO-34 catalyst. *Journal*
645 *of Industrial and Engineering Chemistry*, 18(1), 29–37. doi:10.1016/j.jiec.2011.11.088
- 646 Takahashi, A., Xia, W., Nakamura, I., Shimada, H., & Fujitani, T. (2012). Effects of added
647 phosphorus on conversion of ethanol to propylene over ZSM-5 catalysts. *Applied*
648 *Catalysis A: General*, 423-424, 162–167. doi:10.1016/j.apcata.2012.02.029
- 649 TOTAL. (2008). *MTO / OCP : a strategic research project Testing innovative processes for*
650 *making plastics* (p. 8).
- 651 Ulla, M., Mallada, R., Coronas, J., Gutierrez, L., Miro, E., & Santamaria, J. (2003). Synthesis
652 and characterization of ZSM-5 coatings onto cordierite honeycomb supports. *Applied*
653 *Catalysis A: ...*, 253, 257–269. doi:10.1016/S0926-860X(03)00498-8
- 654 Valle, B., Alonso, a., Atutxa, a., Gayubo, a. G., & Bilbao, J. (2005). Effect of nickel
655 incorporation on the acidity and stability of HZSM-5 zeolite in the MTO process.
656 *Catalysis Today*, 106(1-4), 118–122. doi:10.1016/j.cattod.2005.07.132

- 657 Van Noyen, J., Wilde, A., Schroeven, M., Mullens, S., & Luyten, J. (2012). Ceramic
658 Processing Techniques for Catalyst Design: Formation, Properties, and Catalytic
659 Example of ZSM-5 on 3-Dimensional Fiber Deposition Support Structures. *International*
660 *Journal of Applied Ceramic Technology*, 9(5), 902–910. doi:10.1111/j.1744-
661 7402.2012.02781.x
- 662 Wender, I. (1996). Reactions of synthesis gas. *Fuel Processing Technology*, 48(1996), 189–
663 297. doi:10.1016/S0378-3820(96)01048-X
- 664 Westgård Erichsen, M., Svelle, S., & Olsbye, U. (2013). H-SAPO-5 as methanol-to-olefins
665 (MTO) model catalyst: Towards elucidating the effects of acid strength. *Journal of*
666 *Catalysis*, 298, 94–101. doi:10.1016/j.jcat.2012.11.004
- 667 Wu, W., Guo, W., Xiao, W., & Luo, M. (2011). Dominant reaction pathway for methanol
668 conversion to propene over high silicon H-ZSM-5. *Chemical Engineering Science*,
669 66(20), 4722–4732. doi:10.1016/j.ces.2011.06.036
- 670 Wu, X., & Anthony, R. G. (2001). Effect of feed composition on methanol conversion to light
671 olefins over SAPO-34. *Applied Catalysis A: General*, 218(1-2), 241–250.
672 doi:10.1016/S0926-860X(01)00651-2
- 673 Yang, H., Liu, Z., Gao, H., & Xie, Z. (2010). Synthesis and catalytic performances of
674 hierarchical SAPO-34 monolith. *Journal of Materials Chemistry*, 20(16), 3227.
675 doi:10.1039/b924736j
- 676 Yang, Y., Sun, C., Du, J., Yue, Y., Hua, W., Zhang, C., ... Xu, H. (2012). The synthesis of
677 durable B–Al–ZSM-5 catalysts with tunable acidity for methanol to propylene
678 reaction. *Catalysis Communications*, 24, 44–47. doi:10.1016/j.catcom.2012.03.013
- 679 Yao, J., Zeng, C., Zhang, L., & Xu, N. (2008). Vapor phase transport synthesis of SAPO-34
680 films on cordierite honeycombs. *Materials Chemistry and Physics*, 112, 637–640.
681 doi:10.1016/j.matchemphys.2008.06.019
- 682 Yilmaz, B., & Müller, U. (2009). Catalytic applications of zeolites in chemical industry.
683 *Topics in Catalysis*, 52, 888–895. doi:10.1007/s11244-009-9226-0
- 684 Zamaniyan, A., Mortazavi, Y., Khodadadi, A. A., & Manafi, H. (2010). Tube fitted bulk
685 monolithic catalyst as novel structured reactor for gas–solid reactions. *Applied Catalysis*
686 *A: General*, 385(1-2), 214–223. doi:10.1016/j.apcata.2010.07.014
- 687 Zamaro, J. M., & Miró, E. E. (2010). Novel binderless zeolite-coated monolith reactor for
688 environmental applications. *Chemical Engineering Journal*, 165(2), 701–708.
689 doi:10.1016/j.cej.2010.10.014
- 690 Zamaro, J., Ulla, M., & Miro, E. (2005). Zeolite washcoating onto cordierite honeycomb
691 reactors for environmental applications. *Chemical Engineering Journal*, 106(1), 25–33.
692 doi:10.1016/j.cej.2004.11.003
- 693 Zampieri, A., Kullmann, S., Selvam, T., Bauer, J., Schwieger, W., Sieber, H., ... Greil, P.
694 (2006). Bioinspired Rattan-Derived SiSiC/Zeolite Monoliths: Preparation and

- 695 Characterisation. *Microporous and Mesoporous Materials*, 90(1-3), 162–174.
696 doi:10.1016/j.micromeso.2005.10.049
- 697 Zhu, J., Fan, Y., & Xu, N. (2011). Modified dip-coating method for preparation of pinhole-
698 free ceramic membranes. *Journal of Membrane Science*, 367(1-2), 14–20.
699 doi:10.1016/j.memsci.2010.10.024
- 700 Zhuang, Y., Gao, X., Zhu, Y., & Luo, Z. (2012). CFD modeling of methanol to olefins
701 process in a fixed-bed reactor. *Powder Technology*, 221, 419–430.
702 doi:10.1016/j.powtec.2012.01.041
- 703